Front. Struct. Civ. Eng. 2020, 14(1): 109–122
https://doi.org/10.1007/s11709-019-0579-6

RESEARCH ARTICLE

Using thermodynamic parameters to study self-healing and interface properties of crumb rubber modified asphalt based on molecular dynamics simulation

Dongliang HU[a], Jianzhong PEI[b*], Rui LI[b], Jiupeng ZHANG[b], Yanshun JIA[a], Zepeng FAN[c]

[a] *School of Transportation, Southeast University, Nanjing 211189, China*

[b] *School of Highway, Chang'an University, Xi'an 710064, China*

[c] *School of Transportation Science and Engineering, Harbin Institute of Technology, Harbin 150090, China*

[*] *Corresponding author. E-mail: peijianzhong@126.com*

ABSTRACT The thermodynamic property of asphalt binder is changed by the addition of crumb rubber, which in turn influences the self-healing property as well as the cohesion and adhesion within the asphalt-aggregate system. This study investigated the self-healing and interface properties of crumb rubber modified asphalt (CRMA) using thermodynamic parameters based on the molecular simulation approach. The molecular models of CRMA were built with representative structures of the virgin asphalt and the crumb rubber. The aggregate was represented by SiO_2 and Al_2O_3 crystals. The self-healing capability was evaluated with the thermodynamic parameter wetting time, work of cohesion and diffusivity. The interface properties were evaluated by characterizing the adhesion capability, the debonding potential and the moisture susceptibility of the asphalt-aggregate interface. The self-healing capability of CRMA is found to decrease as the rubber content increases. The asphalt-Al_2O_3 interface with higher rubber content has stronger adhesion and moisture stability. But the influence of crumb rubber on the interfacial properties of asphalt-SiO_2 interface has no statistical significance. Comparing with the interfacial properties of the asphalt-SiO_2 interface, the asphalt-Al_2O_3 interface is found to have a stronger adhesion but a worse moisture susceptibility for its enormous thermodynamic potential for water to displace the asphalt binder.

KEYWORDS crumb rubber modified asphalt, surface free energy, self-healing, interface properties, molecular dynamics simulation

1 Introduction

With the increase of traffic volumes and axle loads in last decade, pavement facilities are liable to damage due to the structural failure caused by the poor properties of raw materials, especially under severe weather conditions and intense ultraviolet radiation [1]. The mechanical properties and durability of pavement materials need to be enhanced to overcome the distressing problem. In terms of flexible pavements, the asphalt binder and mixtures need to reduce brittleness at low temperatures and enhance stiffness at high temperatures, as well as improve moisture stability and aging resistance performance in adverse environments [2,3]. An effective approach is to add polymers to bitumen to generate polymer modified binder with superior combination property [4]. Most polymers used to modify asphalt are newly synthesized, however, crumb rubber recycled from used automobile tires are also widely utilized because it not only improves the asphalt mixture performance in both high temperature and low temperature, but also provides environmental benefits and helps build ecological roads [5–7].

There are two main interaction mechanisms that occur simultaneously in crumb rubber modified asphalt (CRMA): rubber particle swelling and degradation. The swelling is considered to be a nonchemical reaction. Rubber particle absorbs the asphalt's oily phase while

Article history: Received Sep 26, 2018; Accepted Dec 29, 2018

interacting with asphalt binder, forming a gel-like material that is several times its original volume, and leading to the increase of mass viscosity of binder system [8,9]. The rubber degradation is relatively a series of chemical reactions, including the depolymerization and devulcanization that take place when the interaction time is too long or the temperature is too high [10]. Devulcanization is the reverse process of vulcanization by cleaving the crosslink bonds in vulcanized rubber. Depolymerization further breaks the rubber chains into small molecules. Both the processes in turn reduce the binder viscosity. The main problem of CRMA is the separation occurring between the crumb rubber and asphalt binder as the rubber content increases. This separation can be limited by adding certain chemicals to enhance the interaction between crumb rubber and the asphalt binder [11]. The higher viscosity of CRMA during mixing can also be reduced by adding warm mix additive [12,13]. However, as the molecular polarity and potential energy of crumb rubber are different with that of the virgin asphalt, another concern of CRMA is that the addition of crumb rubber has broken the equilibrium of asphalt system and altered the thermodynamic state of asphalt binder [14,15].

The alteration of thermodynamic state of CRMA can be mainly characterized in the change of the surface free energy, which has been successfully used to select materials for asphalt pavement to ensure strong asphalt-aggregate bonds and enhance the pavement performance [16]. Alvarez et al. [17] compared the free energy and energy indices of asphalt rubber and polymer modified asphalt, and concluded that these modified asphalt exhibited significant differences in thermodynamic properties. Tan and Guo [18] found that the virgin asphalt has higher surface free energy compared to the modified asphalt. Bhasin et al. [19] evaluated the bond energy of asphalt-aggregate interfaces formed with asphalt binder modified by SBS and tire rubber. The results demonstrated that the changes of the surface free energy and the energy related parameters varied significantly. The self-healing capability within asphalt mixtures are closely related to the surface free energy of the asphalt, characterized in that the wetting mechanism corresponding to self-healing is determined by the surface free energy [20,21]. In addition, the instantaneous strength gain contributing to the intrinsic healing of crack is governed by this fundamental surface property [22].

The surface free energy also dominates the cohesive bonding of the asphalt-aggregate interface and the adhesive bonding within asphalt binder [16,19]. The adhesion and cohesion in turn affect the resistance of moisture damage and fatigue cracking of asphalt concrete [23,24]. Bhasin et al. [19] used energy parameters to quantify the moisture sensitivity of asphalt concrete with various combinations of the asphalt and aggregate types. They found that the parameters work of adhesion, work of debonding and work of cohesion correlated well with the moisture sensitivity of asphalt mixtures. Kanitpong and Bahia [25] related adhesion and cohesion of asphalt mixtures to the moisture susceptibility in the laboratory, concluded that these energy parameters were good indicators of the asphalt mixture properties. In another research, Bhasin et al. [22] quantified the intrinsic healing rates of asphalt binders using DSR and limitedly verified the results with the work of adhesion. Polymer modifiers were found to improve the adhesion of asphalt binder to the aggregate surface and the cohesion within the binder [26]. However, it is not clear that to what degree the adhesion and cohesion of asphalt binder is influenced with the addition of crumb rubber.

This study aimed to use thermodynamic parameters to investigate the influence of crumb rubber modifier on the self-healing and interface properties of asphalt binder. As the experimental research does not reflect the inherent mechanism of these thermodynamic behaviors, this study was conducted based on the molecular simulations. Molecular dynamics (MD) simulations is widely employed recently to investigate the properties of asphalt materials [27–29]. Zhang and Greenfield [30] developed molecular structures to represent the real asphalt binder and analyzed their density and isothermal compressibility. Bhasin et al. [31] investigated the self-healing mechanisms of asphalt binders using MD approach. Xu and Wang [32] conducted a series of molecular dynamics studies about asphalt binder properties, including oxidative aging effects, moisture damage and cohesion and adhesion behaviors. Guo et al. [33] employed MD to study concentration distribution of asphalt binder on aggregate surface. Wang et al. [34] employed MD approach to investigate micromorphology of asphalt modified by polymer and carbon nanotubes. Most of MD simulations were used to study the performance of neat asphalt binder without modifier and proved to be in good agreement with the experimental results [35,36]. To investigate the modification mechanism of certain additives, MD simulation should be further applied to study the properties of modified asphalt.

This study expected that the self-healing and interface properties of the asphalt binder were affected by crumb rubber modifier and varied regularly with the rubber content. The suggested courses were to:

1) Build molecular models of CRMA with representative structures of asphaltene, naphthene aromatic, saturate fraction, and crumb rubber modifier.

2) Build crack interface models and evaluate the self-healing potential using thermodynamic parameter wetting time, work of cohesion and diffusivity.

3) Build models of asphalt-aggregate interface and asphalt-water-aggregate interface, and evaluate the interface properties by characterizing their adhesion, the thermodynamic potential of debonding and the moisture sensitivity.

2 Model construction

2.1 Force field

A force field is a fundamental energy function used to calculate the potential energy of a system of atoms and model the interatomic interactions in an average mode underlying molecular dynamics simulations. The COMPASS (Condensed-Phase Optimized Molecular Potentials for Atomistic Simulation Studies) force field type was used in this study. COMPASS is an optimized ab initio force field suitable for predicting the properties of common organic molecules, inorganic molecules and polymers, which can be applied at a wide range of pressures and temperatures [37].

The reactive force field (ReaxFF) and coarse-grained (CG) force fields are alternative computational methods for dynamical simulations of bituminous materials to address specific issues that require more elaborate analysis or large length and time scales. ReaxFF is a bond order-based force field of choice to model the chemical reactions by predicting the bond breaking and formation during the simulations [38]. So it is more suitable for simulating asphalt aging or rejuvenating rather than studying the mechanical properties [39]. CG force fields map multiple individual atoms into one CG particle, reducing the degrees of freedom and allowing for much longer simulation times. CG force fields have been practically applied to the characterization of proteins and biomolecular aggregates, as well as predicting the mechanical and thermodynamic properties of polymers or water [40–42]. Considering the complexity of asphalt components that polycyclic aromatic hydrocarbons account for a large proportion of molecular composition, it takes time to accurately derive the CG force field parameters before modeling the mechanical behavior of asphalt using CG potentials. In the next step of this study, the asphalt CG models will be developed to investigate the crack resistance of asphalt materials, which is the inverse characteristic of the self-healing of asphalt.

2.2 Molecular models of CRMA

2.2.1 Molecular structures of CRMA compositions

The molecular models of CRMA and models of asphalt-aggregate interface were built by a commercial molecular simulation software, Accelrys Materials Studio 6.0 [43]. The first step to construct molecular models for CRMA was to select molecular structures that represent the virgin asphalt binder compositions and the crumb rubber modifier. The general methods for simulating the virgin asphalt are choosing three or four different types of molecules as representative asphalt compositions. In this study the asphalt model was constructed following the constituent molecules and weight proportions adopted by Zhang and Greenfield [30]. They used 1,7-dimethylnaphthalene and *n*-docosane (n-$C_{22}H_{46}$) to represent naphthene aromatics and saturates, respectively. Then the asphaltene structure initially proposed by Artok et al. [44] was used, which was a relatively large polycyclic molecular structure compared to the representative structures of naphthene aromatics and saturates. The weight proportion of asphaltenes, naphthene aromatics and saturates was close to 20:20:60. Researchers have conducted many simulations based on these molecular structures of asphalt fractions and verified its reliability [35,45].

In the typical compositions of truck tires, the weight ratio of natural rubber to synthetic rubber is about 1:2, and for automobile tires the weight ratio is 2:1 [46]. Molecular structure of natural rubber was used to represent crumb rubber modifier in this paper. The main component of natural rubber is polyisoprene $(C_5H_8)_n$, which is polymerized from isoprene monomer and has a linear structure [47]. The molecular structures of asphalt compositions and natural crumb rubber are shown in Fig. 1.

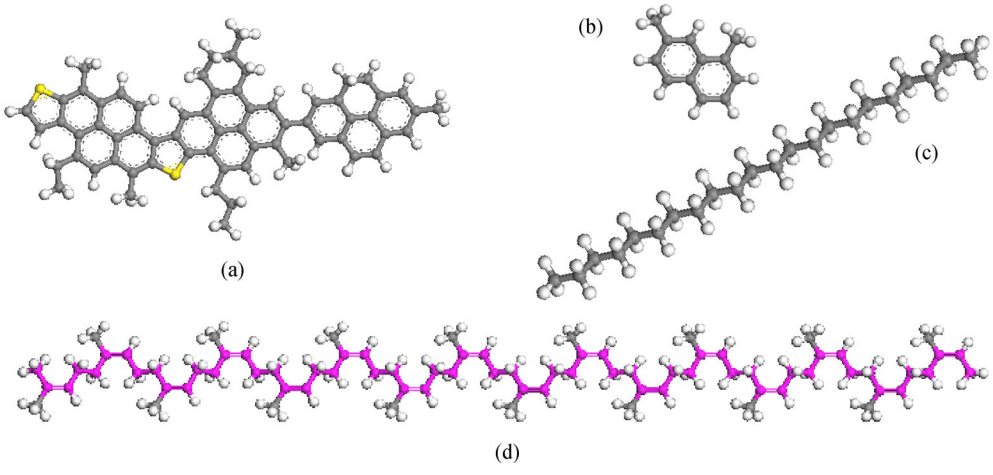

Fig. 1 Molecular structures of CRMA compositions for molecular simulations: (a) asphaltene; (b) naphthene aromatic; (c) saturate; (d) crumb rubber $(C_5H_8)_{16}$.

2.2.2 CRMA models

The virgin asphalt is considered as crumb rubber asphalt with 0% rubber content in the following section. The constituent molecules described above was sketched first before being used to construct the amorphous cells, a representative volume element of CRMA. The amorphous cell is under periodic boundary conditions, indicating that the representative CRMA element is surrounded by its own replicas on all sides.

The molecule number of asphaltenes, naphthene aromatics and saturates in a virgin asphalt binder cell was 5, 27, and 41, respectively, and the corresponding weight ratio was 20.7:19.7:59.6. The crumb rubber contents of CRMB were chosen to be 0%, 5%, 10%, 15%, 20%, and 25% (the weight proportions of crumb rubber to virgin asphalt binder). The weight of the polyisoprene molecular chain with a polymerization degree of 16 is 5.1% of the previously described virgin asphalt binder cell, thereby the polymerization degree of natural crumb rubber molecular chain was chosen to be 16 and the number of molecular chains added to the CRMA cell was 1 to 5, corresponding to 5% to 25% of the dosages of crumb rubber. The target density of CRMA was set to 1 g/cm^3, which would be adjusted during the dynamics process. The temperature was set to 298K, and the lattice type of amorphous cell was set to cubic. The Ewald summation method was applied for electrostatic interactions and the atom-based summation method was applied for the van der Waals interactions with a cutoff distance of 15.5 Å.

The newly built cell did not represent the real molecular conformation of asphalt binder because it was not in the lowest energy state. To achieve energy minimization, the initial configuration was subjected to geometry optimization with 10000 iterations in the Forcite-calculation module. The optimized configuration was further refined by performing Forcite dynamic calculations in the canonical ensemble (NVT ensemble) for 500 ps at 453K and then in isothermal-isobaric ensemble (NPT ensemble) for 500 ps at 453K and 1 atm pressure to ensure that the system reached equilibrium. Then the Forcite quench calculation was carried out on the equilibrium system to reduce the system temperature from 453K to 298K with simulation time of 100 ps.Thus the obtained stable configuration was able to represent the real CRMA and then used for further calculation and analysis. The molecular model of CRMA is shown in Fig. 2, where the crumb rubber molecules are highlighted.

To verify whether the constructed models can represent the real asphalt, the calculated density results and the experimentally measured values of virgin asphalt at different temperatures were compared in Fig. 3. The calculated values are consistent with simulation results in previous literatures, but there is a difference from the experimental measured data [30,48,49]. The reason for the difference might be that some components of the real asphalt, such as wax, were not represented in the MD model. Moreover, the molecular weight of the three asphalt components adopted in this study was small compared to the representative molecular structures for the asphalt SARA fractions [50]. However, the asphalt density results show a significant temperature dependence, which is consistent with the experimental measured results. Therefore, it is reasonable to believe that MD simulations can model the thermodynamic properties of asphalt with a certain deviation.

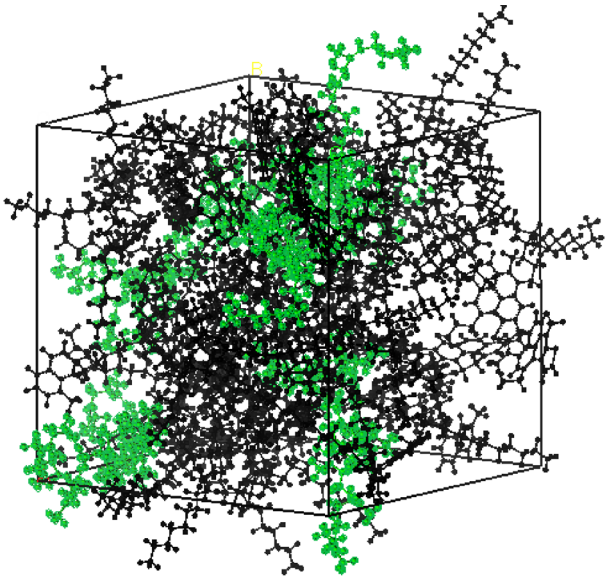

Fig. 2 Molecular model of CRMA; the crumb rubber molecules are highlighted.

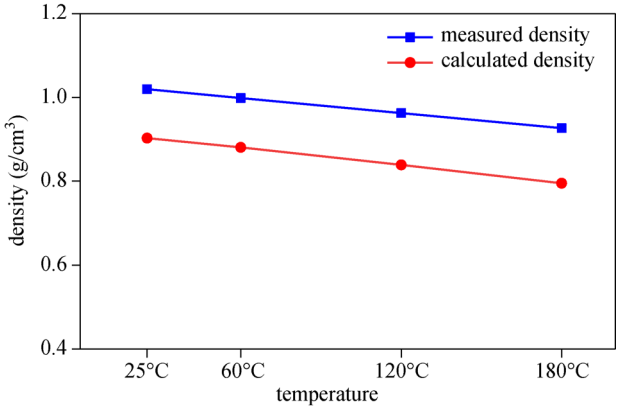

Fig. 3 Comparison between calculated densities of asphalt binder from MD simulations and the experimentally measured results.

2.3 Models of crack interface

The asphalt binder models with a crack interface were created before studying their self-healing properties, which was achieved by building layered structure in build layers module. The binder model with a crack consists of two

layers, where the layer1 and layer2 are the same one of the stable configurations previously described. A 10 Å vacuum pad was added between layer1 and layer2 to represent crack interface, as shown in Fig. 4. If the selected stable configuration represents CRMA with 5% crumb rubber, then the obtained layered structure represents 5% rubber content CRMA with a 10 Å crack.

2.4 Models of asphalt-aggregate interface

Silicon dioxide (SiO_2) and aluminum oxide (Al_2O_3) are the most common compounds in aggregate materials used in asphalt mixture. In this paper SiO_2 and Al_2O_3 were selected to represent aggregate to construct asphalt-aggregate interface models for analysis of the adhesion properties. Taking the creation of asphalt-SiO_2 interface model as an example, the first step was to import the unit cell of α-quartz SiO_2 from software database, and then cleaved the (1 1 0) plane to obtain a SiO_2 surface. As the non-bond cutoff distances are 15.5 Å in the force field calculation setting, the thickness of the cleaved SiO_2 crystal must be more than 15.5 Å to ensure the accuracy of simulation. Thus the thickness was chosen to be 17.196 Å in this study, seven times the length of the OC dimension of the cleaved quartz. Then the SiO_2 surface was used to create a supercell by increasing the supercell range to 4 and 7 for U and V, respectively. After performing the build vacuum slab crystal process with the vacuum thickness set to 0.0, a three-dimensional SiO_2 crystal was obtained.

Confined asphalt layers containing various rubber contents were constructed in orthorhombic lattice type to create asphalt-SiO_2 interface model. The axial lengths of a and b of the confined asphalt layer were set to be the same as the SiO_2 crystal. The confined asphalt layers were subjected to geometry optimization with 10000 iterations, followed by Forcite dynamic calculations in the NPT ensemble for 200 ps at 298K and 1 atm pressure to reach equilibrium. The other simulation conditions were consistent with the simulations for the amorphous cells.

The asphalt-SiO_2 interface model was created by using the layer builder. The SiO_2 crystal subjected to energy minimization was selected as layer1 and the confined asphalt layer was selected as layer2. A 30 Å vacuum was inserted outside the layer2 to eliminate the effects of boundary condition. Before performing the next simulation, it is necessary to fix the SiO_2 crystal and then run the energy minimization calculation. The creation of asphalt-Al_2O_3 interface model is similar to the above process. It should be noted that Al_2O_3 is an ionic compound, so the crystal bonds must be removed to ensure the calculation accuracy. The detailed steps can be found by viewing the software tutorial. The asphalt-SiO_2 interface model and asphalt-Al_2O_3 interface model are shown in Fig. 5.

2.5 Models of asphalt-water-aggregate interface

Because the silica solid surface is easily hydroxylated in presence of water [32,51], the surface of SiO_2 crystal in asphalt-water-aggregate interface model was fully hydroxylated and it was characterized by 8.71 OH/nm^2 in this study. The schematic representation of the fully hydroxylated silica surface is given in Fig. 6.

The asphalt-water-aggregate interface model used to study moisture susceptibility consists of three layers. Layer1 is SiO_2 or Al_2O_3 crystal and layer3 is the confined asphalt layer. Layer2 is a confined water layer, which consists of 300 water molecules with a density of 1 g/cm^3 and a size of 38 Å × 34.5 Å × 6.84 Å。 A 30 Å vacuum is also inserted outside layer 3. The built layered structure needs to perform the energy minimization calculation. The asphalt-water-aggregate interface models are shown in Fig. 7.

3 Thermodynamic parameters related to self-healing and interface properties

3.1 Parameters related to self-healing

Mechanism corresponding to self-healing in asphalt

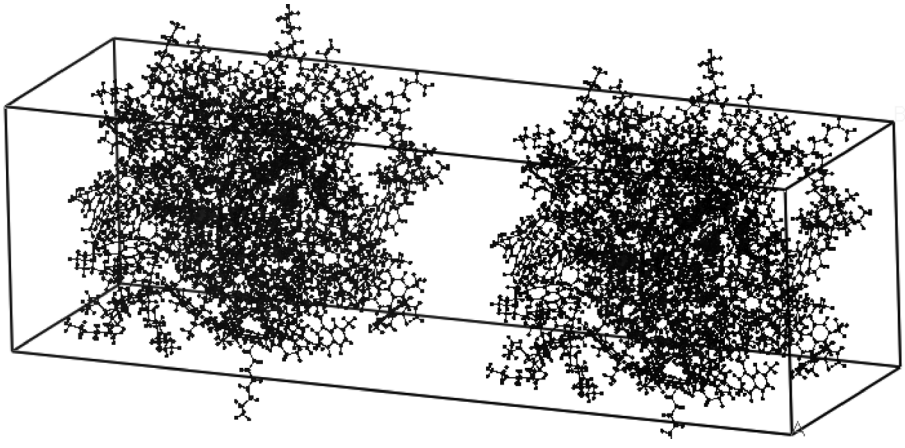

Fig. 4 Molecular models of CRMA with a 10 Å crack.

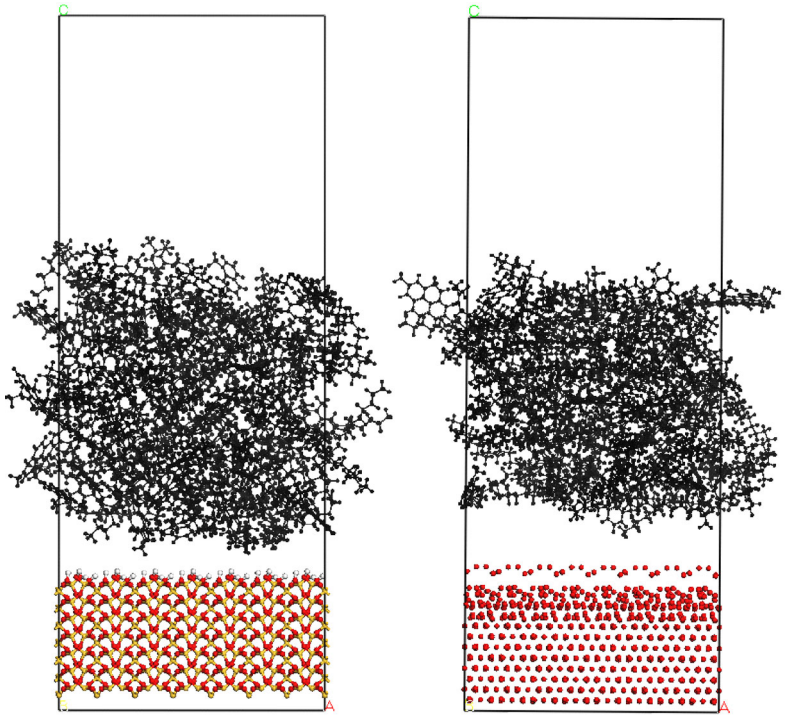

Fig. 5 Molecular models of asphalt-aggregate interface: (a) asphalt-SiO_2 interface; (b) asphalt-Al_2O_3 interface.

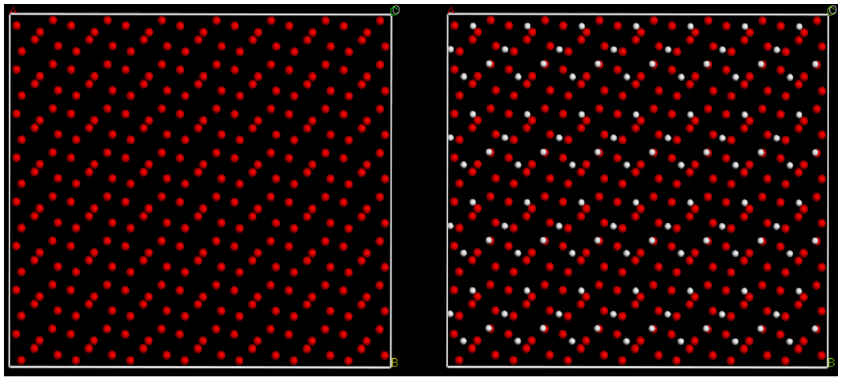

Fig. 6 Schematic representation of silica surface from the top view: (a) nonhydroxylated; (b) fully hydroxylated. The silicon atoms and bonds are deleted. Red and white atoms are hydrogen and oxygen atoms, respectively.

materials can be classified into two categories: wetting and intrinsic healing [22]. The theory was proposed by Bhasin et al. on the basis of Wool and Schapery's work about self-healing in polymers and other viscoelastic materials [52,53]. The wetting is determined by the surface free energy and other material properties of asphalt binder. The intrinsic healing can be further considered to be a combination of two mechanisms. The first is an instantaneous but limited strength gain at the moment when the cracked surface are in contact due to the cohesion work of the crack interface [22]. The second is the lasting interfacial strength after the cracked surfaces have cohered, which is dominated by the diffusivity of molecules around the crack.

1) Thus the wetting time defined as the simulation time when the cracked surface were in contact was used to evaluate the crack wetting rate.

2) The work of cohesion between the crack surfaces and the diffusivity of asphalt molecules were used to evaluate the capability of intrinsic healing.

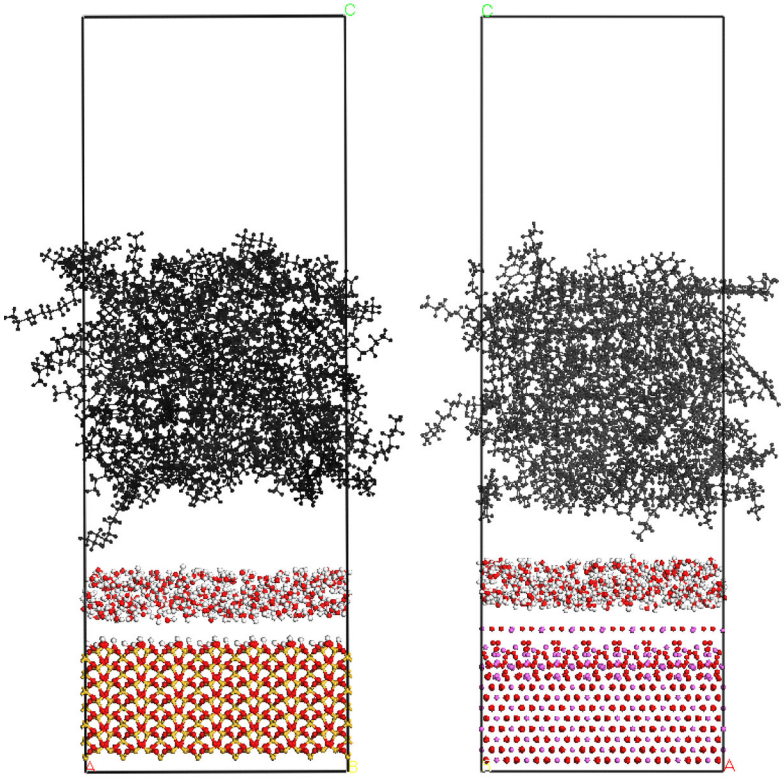

Fig. 7 Molecular models of asphalt-water-aggregate interface: (a) asphalt-water-SiO_2 interface; (b) asphalt-water-Al_2O_3 interface.

The wetting and intrinsic healing of crack interface can be simulated by molecular dynamics approach based on the models created previously. The specific steps were introduced in next section.

3.2 Parameters related to adhesion

When the asphalt binder in asphalt concrete are separated from its interface with the aggregate, the surface free energy of system is increased due to the formation of new surfaces. The difference between the energy of the system before and after the separation is the interface energy between asphalt and aggregate. The system needs to absorb energy from the outside during the separating process. Work of adhesion is the work required to separate the asphalt binder and aggregate from their interface [16].

Work of adhesion was used to evaluate the adhesion capacity of adhesion between asphalt and aggregate. A higher magnitude of work of adhesion indicates the superior adhesion between the asphalt binder and aggregate.

3.3 Parameters related to moisture sensitivity

Due to the hydrophilic nature of mineral and the hydrophobic nature of bitumen, water tends to displace asphalt binder from the aggregate surface and to form an asphalt-water interface and an aggregate-water interface [54]. The total energy of the system is lower in this new state, therefore, the debonding process dissipates energy to the outside and the dissipated energy is the so-called work of debonding [16].

As previously described, the magnitude of work of adhesion (W_{adhesion}) is proportional to the resistance to the separation of the asphalt binder and aggregate, and the magnitude of work of debonding ($W_{\text{debonding}}$) is inversely proportional to the resistance to the displacement of asphalt binder by water from the surface of the aggregate. Accordingly, the parameter energy ratio (ER) obtained by dividing W_{adhesion} by $W_{\text{debonding}}$ can be used to directly evaluate the moisture resistance of the asphalt concrete as follow [16]:

$$ER = \frac{W_{\text{adhesion}}}{W_{\text{debonding}}}. \tag{1}$$

Thus work of debonding and energy ratio were used to evaluate moisture sensitivity. A higher magnitude of work of debonding indicates a higher thermodynamic potential for water to displace asphalt binder from the surface of aggregate. A higher magnitude of energy ratio implies that the asphalt concrete is less sensitive to moisture damage, and vice versa.

4 Results and discussion

4.1 Self-healing of crack interface

4.1.1 Dynamic simulation of self-healing

The dynamic simulations in this study were conducted using Accelrys Materials Studio 6.0. For the wetting simulation, the binder model with a cracks was subjected to a Forcite dynamics calculation for 100 ps in NPT ensemble at 298K and 1 atm pressure. A trajectory document containing continuously changing configurations was obtained. By playing the configuration animation on the trajectory document, it can be observed that the crack surfaces are gradually approaching, and the volume of the cell continues to decrease until the surfaces are in close contact and the cell volume does not change significantly. This process represents the wetting of asphalt crack interface. The wetting time was obtained by recording the simulation time when the system density reaches a stable value. The changes of density and configuration of CRMA model with a crack are shown in the Fig. 8.

The stable configuration after crack wetting was extracted to represent the wetted crack interface, which was subjected to a further Forcite dynamics calculation for 200 ps in NVT ensemble at 298K to simulate the intrinsic healing. The resulting structure was a healed binder model and used to calculate work of cohesion. The work of cohesion is the numerically sum of surface free energy of the surfaces of asphalt crack. Since the wetting process is also a function of the surface free energy as previously described, the wetting time and the work of adhesion are not independent parameters, but this does not affect their application to evaluate the self-healing properties of asphalt binder. The surface free energy is defined as the work required to build a unit area of a particular surface [16], which cannot be calculated directly in the software, however, the work of cohesion can be calculated by using the following equation:

$$W_{\text{cohesion}} = (E_{\text{layer1}} + E_{\text{layer2}}) - E_{\text{total}}, \tag{2}$$

where W_{cohesion} is the work of cohesion between the asphalt crack surfaces; E_{total} is the total potential energy of the healed binder model; E_{layer1} is the potential energy of the layer1 without the layer2; E_{layer2} is the potential energy of the layer2 without the layer1. E_{total} was obtained by performing a Forcite energy calculation for the healed binder model. Duplicating the healed binder model and deleting the layer2, the remaining layer1 was used to calculate E_{layer1} by performing a Forcite energy process again. E_{layer2} was calculated by the same way.

The term diffusivity refers to the random motion of particles due to the particle diffusion and the concentration gradient, which is defined as follows [48]:

$$D = \frac{1}{6N}\lim_{t\to\infty}\frac{\mathrm{d}}{\mathrm{d}t}\sum_{n=1}^{N}[x_n(t) - x_n(0)]^2, \tag{3}$$

where D is the diffusivity; N is the number of particles to be averaged; $x_n(0)$ is the original position of each particle; $x_n(t)$ is the position of each particle at a specific time. Diffusivity in this paper is used to analyzing the transportation of binder molecules.

Diffusivity determines the increase of mean square displacement (MSD), which is defined as the deviation of the position of particles with respect to the original positions for a given time as follows [55]:

$$\text{MSD} = \frac{1}{N}\sum_{n=1}^{N}[x_n(t) - x_n(0)]^2, \tag{4}$$

where the terms are the same as Eq. (2). In this software, MSD can be obtained by performing Forcite MSD analysis for the obtained trajectory document.

It is important to realize that when performing dynamics

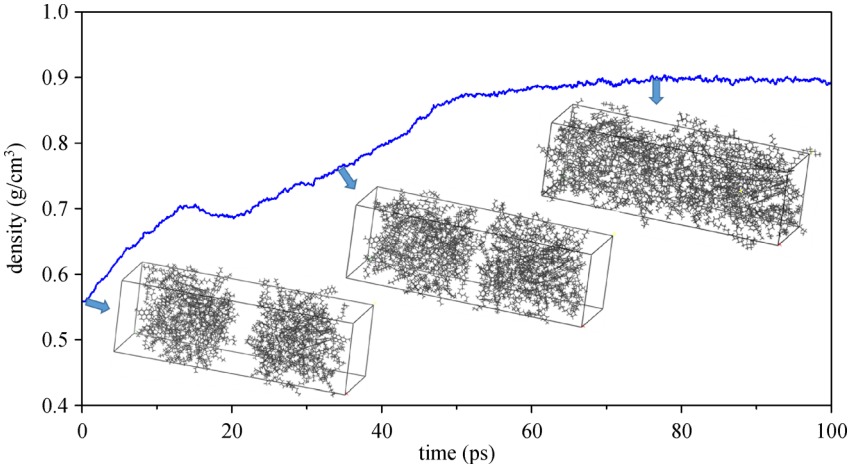

Fig. 8 The changes of density and configuration of CRMA model with crack. (simulation under NPT ensemble at 298K and 1 atm)

calculations under NPT ensemble, the system volume is gradually reduced, and the asphalt molecules move toward the coordinate origin at the same time as self-diffusion. The binder molecule with a larger distance from the coordinate origin moves further distance, therefore, MSD of layer1 and layer2 are significantly different because the coordinate origin is outside the layer1 and is far away from layer2. To eliminate this effects, the coordinate origin of crack interface model needs to be set in the middle of the crack by moving the positions of the layered structure.

According to the above definition, the diffusivity D can be simplified as follows:

$$D = \frac{a}{6}, \tag{5}$$

where a is the slop of the fitting straight line of MSN with respect to time. The unit of a is Å^2/ps. Because the values of MSD do not increase linearly in the initial stage of the simulation, and often subject to large fluctuations at the end as the statistical accuracy decreases with the time interval, the initial nonlinear part and the second half of the MSD data were deleted in the fitting. Figure 9 shows the MSD and the linear fitting for CRMA molecules around the crack surfaces.

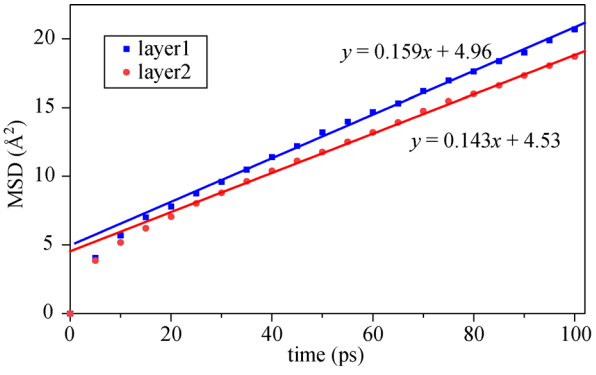

Fig. 9 MSD plotting and the linear fitting for virgin asphalt binder molecules around the crack surfaces.

4.1.2 Self-healing capability of CRMA

Figure 10 shows the wetting time of crack healing for asphalt binder with different crumb rubber contents. The plotting records the mean values and the standard error of the mean of three independent simulations. Except special explanations, all the following figures record the mean values and the corresponding standard error for three simulations. It can be seen that the wetting time increases dramatically with the rise of rubber content, which means the first step of self-healing is held back by the addition of crumb rubber. When the rubber content changes from 0% to 25%, the wetting time increases from 40 ps to 85 ps, namely the wetting rate has dropped more than 50%. Figure 11 shows the work of cohesion between the crack surfaces of CRMA as a function of rubber content. As the crumb rubber content increases, the work of adhesion shows a statistical upward trend, indicating that the addition of crumb rubber enhances the intrinsic propensity of asphalt crack healing. However, the tendency of work of adhesion is opposite to that of the wetting rates, which verifies that in addition to the work of cohesion (or the surface free energy), wetting process of asphalt crack is also determined by other material attributes, and it can even be inferred that other factors have a greater impact than the work of cohesion. In addition, the tendency of work of adhesion indicates that the crack resistance of asphalt binder is improved after the crumb rubber is added.

Figure 12 plots the diffusivity of asphalt molecules around the crack surfaces of CRMA obtained from six samples. It can be observed that the addition of crumb rubber suppresses the diffusivity of asphalt binder. The diffusivity of CRMA with 25% rubber content decreases by about 25% compared to that of the virgin asphalt. As summarized in Figs. 10–12, the addition of crumb rubber significantly degrades the self-healing capability of asphalt binder, although the intrinsic healing tendency increased to some extent. Literature reported that increased rubber content deteriorated the healing capability of CRMA, which was consistent with the findings in this section [56]. In this study, the degradation of self-healing capability was characterized by increasing the wetting time of asphalt crack and restraining the diffusivity of asphalt molecules. The further factors are the changes of material characteristics such as viscoelastic and mechanical properties. As previously introduced, the asphalt composition changes when rubber particle interacts with asphalt binder and absorbs the asphalt's oily phase, which also affects the self-healing capacity. This paper cannot figure out which factor mainly affects the self-healing deterioration, and it needs to be researched in the following study.

4.2 Adhesion of CRMA-aggregate interface

4.2.1 Dynamic simulation of adhesion

The asphalt-aggregate interface model were subjected to Forcite dynamics calculation for 100 ps in NVT ensemble at 298K after energy minimization with 5000 iterations. The obtained asphalt-aggregate interface model represents the equilibrium interface state where asphalt binder and aggregate are completely adhered. Based on the obtained asphalt-aggregate model, the work of adhesion between asphalt and aggregate was calculated as follows:

$$E_{\text{inter\_aag}} = E_{\text{aag}} - (E_{\text{a}} + E_{\text{ag}}), \tag{6}$$

$$W_{\text{adhesion}} = -E_{\text{inter\_aag}} = (E_{\text{a}} + E_{\text{ag}}) - E_{\text{aag}}, \tag{7}$$

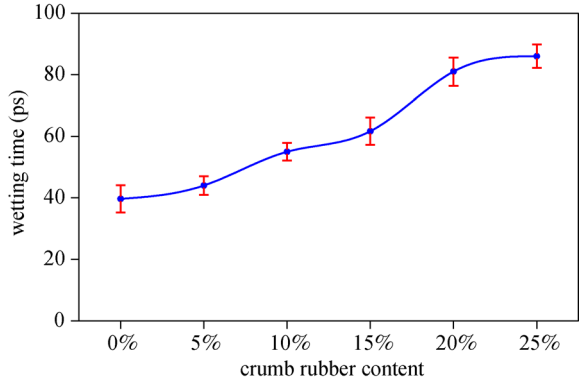

Fig. 10 Wetting time of crack healing of CRMA.

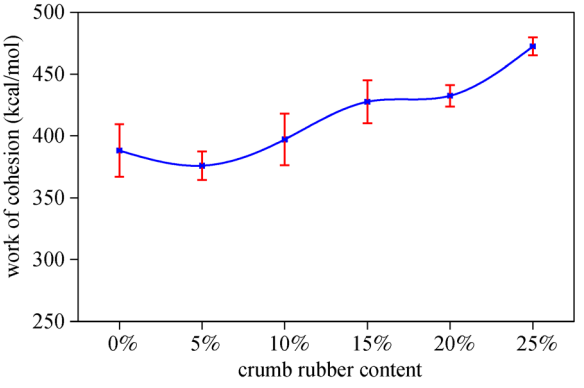

Fig. 11 Work of cohesion between the crack surfaces of CRMA.

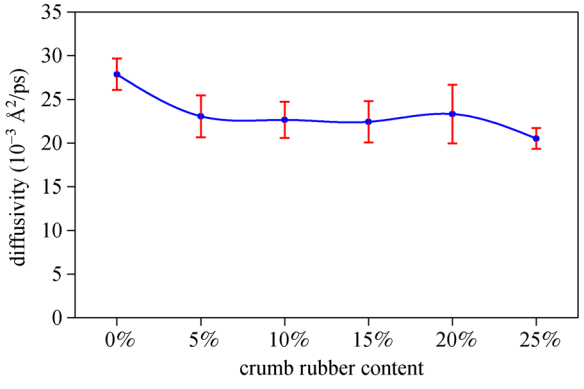

Fig. 12 Diffusivity of molecules around the crack surfaces of CRMA.

where $E_{\text{inter\_aag}}$ is the interaction energy between asphalt and aggregate; W_{adhesion} is the work of adhesion between asphalt and aggregate; E_{agg} is the total potential energy of the obtained asphalt-aggregate interface model after dynamics process; E_{a} is the potential energy of the asphalt binder without the aggregate; E_{ag} is the potential energy of the aggregate without the asphalt binder. E_{agg}, E_{a}, and E_{ag} were obtained by performing Forcite energy calculations after releasing the fixed crystals. The obtained $E_{\text{inter\_aag}}$ is a negative value, indicating that the asphalt binder is binding to aggregate.

4.2.2 Adhesion between CRMA and aggregate

The work of adhesion between the aggregate and CRMA is presented in Fig. 13. Figure 13(a) shows the work of adhesion between Al_2O_3 and CRMA ($W_{\text{adh}}^{\text{asp\_Al}_2\text{O}_3}$) as an increasing function of rubber content. As the rubber content is up to 25%, the work of adhesion grows from 1200 to 1500 kcal/mol, implying that the adhesion between Al_2O_3 and asphalt binder is enhanced by adding crumb rubber, which might attribute to the increase of asphalt viscosity caused by rubber particle swelling. Figure 13(b) shows the work of adhesion between SiO_2 and CRMA ($W_{\text{adh}}^{\text{asp\_SiO}_2}$) of three simulations, which fluctuates between 200 and 230 kcal/mol as the rubber content changes. However, there is no obvious change regular of $W_{\text{adh}}^{\text{asp\_SiO}_2}$ with the rise of rubber content. The likely explanation is as follow: the magnitude of $W_{\text{adh}}^{\text{asp\_SiO}_2}$ is small and the change of $W_{\text{adh}}^{\text{asp\_SiO}_2}$ driven by crumb rubber is little, thus the change regular is covered up by the systematic error of the simulations. To accurately observe the change law of $W_{\text{adh}}^{\text{asp\_SiO}_2}$, it is necessary to reduce the influence of the systematic error by expanding the contact area of the asphalt binder and the aggregate in simulations, but this will be much more computationally expensive. Therefore, further analysis should be conducted using the aforementioned CG potentials.

Note that $W_{\text{adh}}^{\text{asp\_Al}_2\text{O}_3}$ is much larger than $W_{\text{adh}}^{\text{asp\_SiO}_2}$ regardless of the influence of crumb rubber. This is because SiO_2 is an acidic compound and Al_2O_3 is an amphoteric compound, while the weakly acidic bitumen has a stronger adhesion with amphoteric compounds than acidic compounds.

4.3 Moisture sensitivity of CRMA-aggregate interface

4.3.1 Dynamic simulation of debonding

The asphalt-water-aggregate interface model was subjected to Forcite dynamics calculation for 100 ps in NVT ensemble at 298K after energy minimization with 5000 iterations. The obtained asphalt-water-aggregate interface model represents the state where water fully infiltrates the interface between the asphalt binder and aggregate. Based on the obtained asphalt-water-aggregate model, the work of debonding for water to displace asphalt binder from its interface with aggregate was calculated according to Eq. (8) and ER was calculated according to Eq. (1).

$$W_{\text{debonding}} = E_{\text{inter\_aag}} - (E_{\text{inter\_aw}} + E_{\text{inter\_agw}}), \quad (8)$$

where $W_{\text{debonding}}$ is the work of debonding; $E_{\text{inter\_aag}}$ is the

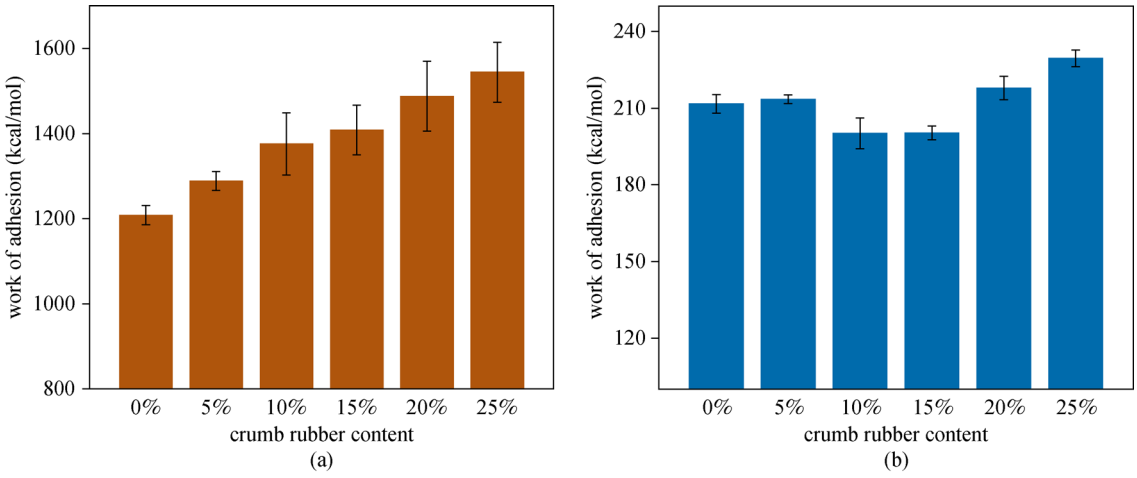

Fig. 13 The work of adhesion between the aggregate and CRMA: (a) work of adhesion between Al_2O_3 and CRMA; (b) work of adhesion between SiO_2 and CRMA.

interaction energy between asphalt and aggregate; E_{inter_aw} is the interaction energy between asphalt and water; E_{inter_agw} is the interaction energy between aggregate and water. The acquisition of E_{inter_aw} and E_{inter_agw} were in the same way as Eq. (6).

4.3.2 Moisture sensitivity between CRMA and aggregate

Figure 14 illustrates the work of debonding ($W_{deb}^{asp\_Al_2O_3}$) and the energy ratio ($ER^{asp\_Al_2O_3}$) of asphalt-Al_2O_3 interface. The plotting shows that $W_{deb}^{asp\_Al_2O_3}$ varies around 14000 kcal/mol, much larger than $W_{deb}^{asp\_Al_2O_3}$, indicating the thermodynamic potential for water to displace asphalt binder from the Al_2O_3 surface is huge. However, $W_{deb}^{asp\_Al_2O_3}$ does not show an obvious rising trend or downtrend with the increase of rubber content. The explanation is as follow: the large magnitude of $W_{deb}^{asp\_Al_2O_3}$ is mainly attributed to the hydrophilic property of Al_2O_3 rather than the hydrophilicity of bitumen or the weak adhesion between bitumen and Al_2O_3, but the influence of crumb rubber cannot affect the hydrophilic property of Al_2O_3, thus $W_{deb}^{asp\_Al_2O_3}$ does not show a correlation with the rubber content. Because the degree of change of $W_{deb}^{asp\_Al_2O_3}$ is much larger than $W_{adh}^{asp\_Al_2O_3}$, the parameter $ER^{asp\_Al_2O_3}$ shows the same growth trend as $W_{adh}^{asp\_Al_2O_3}$ exhibits, indicating that the asphalt concrete with higher rubber content is less sensitive to moisture damage.

Figure 15 illustrates the work of debonding ($W_{deb}^{asp\_SiO_2}$) and the energy ratio ($ER^{asp\_SiO_2}$) of asphalt-SiO_2 interface. Similar to the work of adhesion between asphalt binder and

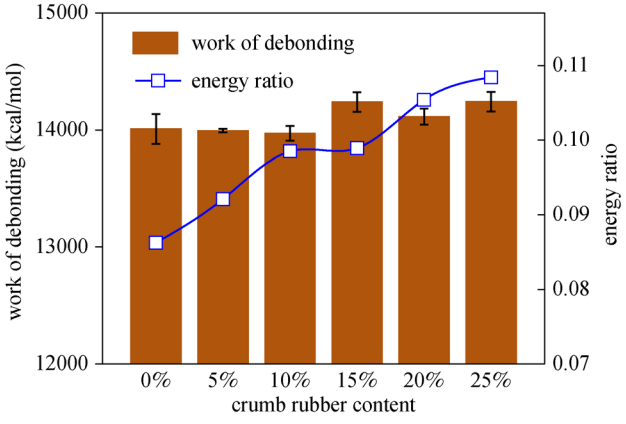

Fig. 14 The work of debonding and the energy ratio (*ER*) of asphalt-Al_2O_3 interface.

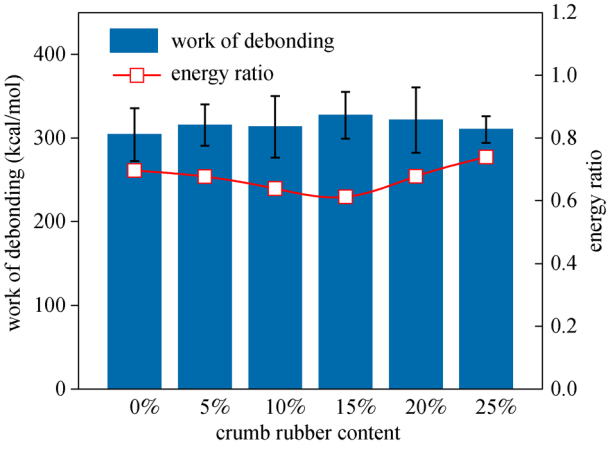

Fig. 15 The work of debonding and the energy ratio of asphalt-SiO_2 interface.

SiO_2, $W_{deb}^{asp\_SiO_2}$ is also affected by the systematic error of the simulations and exhibits no variation regular with the rise of rubber, thus $ER^{asp\_SiO_2}$ is not statistically significant. Nonetheless, it can be observed that $W_{deb}^{asp\_SiO_2}$ is much smaller than $W_{deb}^{asp\_Al_2O_3}$, and $ER^{asp\_SiO_2}$ is larger than $ER^{asp\_Al_2O_3}$, suggesting that the asphalt-SiO_2 interface has a better moisture stability than the asphalt-Al_2O_3 interface. However, it is not clear to what extent this result reveals the moisture susceptibility of the asphalt-Al_2O_3 interface and asphalt-SiO_2 interface, thus the conclusion could not be further derived before being verified by the experimental study.

5 Conclusions

The self-healing capability was evaluated with the parameters wetting time, work of cohesion and diffusivity. The interface properties of asphalt binder and aggregate was evaluated using the work of adhesion, the work of debonding and the parameter energy ratio, corresponding to characterize the adhesion capability, the thermodynamic potential of debonding and the moisture susceptibility of the asphalt-aggregate interface. Based on the results of the molecular dynamics simulation, the self-healing capability of asphalt binder is found to decrease as the rubber content increases, which is manifested by the prolongation of the wetting time of crack healing and the decline of the diffusivity of asphalt molecules. The deteriorated self-healing capability is mainly attributed to the changes of material characteristics such as viscoelastic and mechanical properties other than the change of the surface free energy.

The adhesion between the asphalt binder and Al_2O_3 increases with the rise of rubber content, but the thermodynamic potential for water to displace asphalt binder from the Al_2O_3 surface is not affected by the addition of crumb rubber, thus the asphalt- Al_2O_3 interface of asphalt concrete with higher rubber content has a stronger moisture stability. As the influence of crumb rubber on the interfacial properties of asphalt-SiO_2 interface is covered up by the systematic error of the simulations, the change of asphalt-SiO_2 interfacial properties with the rising of rubber content has no statistical significance. By comparing with the interfacial properties of the asphalt-SiO_2 interface, the asphalt-Al_2O_3 interface is found to have a stronger adhesion but a worse moisture susceptibility for its enormous thermodynamic potential for water to displace the asphalt binder.

Acknowledgements This study was supported by the Special Fund for Basic Scientific Research of Central College of Chang'an University (Nos. 300102218405, 300102218413, and 310821153502), and the Department of Science & Technology of Shaanxi Province (Nos. 2016ZDJC-24 and 2017KCT-13).

References

1. Zhang J, Cui S, Cai J, Pei J, Jia Y. Life-cycle reliability evaluation of semi-rigid materials based on modulus degradation model. KSCE Journal of Civil Engineering, 2018, 22(6): 2043–2054
2. Nejad F M, Aghajani P, Modarres A, Firoozifar H. Investigating the properties of crumb rubber modified bitumen using classic and SHRP testing methods. Construction & Building Materials, 2012, 26(1): 481–489
3. Li R, Dai Y, Wang P, Sun C, Zhang J, Pei J. Evaluation of Nano-ZnO dispersed state in bitumen with digital imaging processing techniques. Journal of Testing and Evaluation, 2017, 46(3): 20160401
4. Yildirim Y. Polymer modified asphalt binders. Construction & Building Materials, 2007, 21(1): 66–72
5. Lo Presti D. Recycled Tyre Rubber Modified Bitumens for road asphalt mixtures: A literature review. Construction & Building Materials, 2013, 49: 863–881
6. Xiao F, Yao S, Wang J, Wei J, Amirkhanian S. Physical and chemical properties of plasma treated crumb rubbers and high temperature characteristics of their rubberised asphalt binders. Road Materials and Pavement Design, 2018 (in press)
7. Li R, Yu Y, Zhou B, Guo Q, Li M, Pei J. Harvesting energy from pavement based on piezoelectric effects: Fabrication and electric properties of piezoelectric vibrator. Journal of Renewable and Sustainable Energy, 2018, 10(5): 054701
8. Abdelrahman M, Carpenter S. Mechanism of interaction of asphalt cement with crumb rubber modifier. Transportation Research Record: Journal of the Transportation Research Board, 1999, 1661(1): 106–113
9. Shu X, Huang B. Recycling of waste tire rubber in asphalt and Portland cement concrete: An overview. Construction & Building Materials, 2014, 67: 217–224
10. Zanzotto L, Kennepohl G. Development of rubber and asphalt binders by depolymerization and devulcanization of scrap tires in asphalt. Transportation Research Record: Journal of the Transportation Research Board, 1996, 1530(1): 51–58
11. Mull M, Stuart K, Yehia A. Fracture resistance characterization of chemically modified crumb rubber asphalt pavement. Journal of Materials Science, 2002, 37(3): 557–566
12. Yu H, Leng Z, Zhou Z, Shih K, Xiao F, Gao Z. Optimization of preparation procedure of liquid warm mix additive modified asphalt rubber. Journal of Cleaner Production, 2017, 141: 336–345
13. Li R, Wang C, Wang P, Pei J. Preparation of a novel flow improver and its viscosity-reducing effect on bitumen. Fuel, 2016, 181: 935–941
14. Wang S, Yuan C, Jiaxi D. Crumb tire rubber and polyethylene mutually stabilized in asphalt by screw extrusion. Journal of Applied Polymer Science, 2014, 131(23): 81–86
15. Sultana S, Bhasin A. Effect of chemical composition on rheology and mechanical properties of asphalt binder. Construction & Building Materials, 2014, 72: 293–300
16. Bhasin A, Little D N, Vasconcelos K L, Masad E. Surface free energy to identify moisture sensitivity of materials for asphalt mixes. Transportation Research Record: Journal of the Transportation

Research Board, 2007, 2001(1): 37–45
17. Alvarez A E, Ovalles E, Epps Martin A. Comparison of asphalt rubber-aggregate and polymer modified asphalt-aggregate systems in terms of surface free energy and energy indices. Construction & Building Materials, 2012, 35: 385–392
18. Tan Y, Guo M. Using surface free energy method to study the cohesion and adhesion of asphalt mastic. Construction & Building Materials, 2013, 47: 254–260
19. Bhasin A, Howson J, Masad E, Little D, Lytton R. Effect of modification processes on bond energy of asphalt binders. Transportation Research Record: Journal of the Transportation Research Board, 2007, 1998(1): 29–37
20. Cheng D, Little D, Lytton R, Holste J. Surface energy measurement of asphalt and its application to predicting fatigue and healing in asphalt mixtures. Transportation Research Record: Journal of the Transportation Research Board, 2002, 1810(1): 44–53
21. Sun D, Sun G, Zhu X, Guarin A, Li B, Dai Z, Ling J. A comprehensive review on self-healing of asphalt materials: Mechanism, model, characterization and enhancement. Advances in Colloid and Interface Science, 2018, 256: 65–93
22. Bhasin A, Bommavaram D, Greenfiled M. Intrinsic healing in asphalt binders—Measurement and impact of molecular morphology. In: The 6th International Conference on Maintenance and Rehabilitation of Pavements and Technological Control. Torino: Turin Polytechnic, 2009
23. Zhang J, Fan Z, Hu D, Hu Z, Pei J, Kong W. Evaluation of asphalt-aggregate interaction based on the rheological properties. International Journal of Pavement Engineering, 2018, 19(7): 586–592
24. Bhasin A, Little D N, Bommavaram R, Vasconcelos K. A framework to quantify the effect of healing in bituminous materials using material properties. Road Materials and Pavement Design, 2008, 9(sup1): 219–242
25. Kanitpong K, Bahia H. Relating adhesion and cohesion of asphalts to the effect of moisture on laboratory performance of asphalt mixtures. Transportation Research Record: Journal of the Transportation Research Board, 2005, 1901(1): 33–43
26. Kök B V, Çolak H. Laboratory comparison of the crumb-rubber and SBS modified bitumen and hot mix asphalt. Construction & Building Materials, 2011, 25(8): 3204–3212
27. Qu X, Liu Q, Guo M, Wang D, Oeser M. Study on the effect of aging on physical properties of asphalt binder from a microscale perspective. Construction & Building Materials, 2018, 187: 718–729
28. Li R, Guo Q, Du H, Pei J. Mechanical property and analysis of asphalt components based on molecular dynamics simulation. Journal of Chemistry, 2017, 2017: 1531632
29. Chen Z, Pei J, Li R, Xiao F. Performance characteristics of asphalt materials based on molecular dynamics simulation—A review. Construction & Building Materials, 2018, 189: 695–710
30. Zhang L, Greenfield M L. Analyzing properties of model asphalts using molecular simulation. Energy & Fuels, 2007, 21(3): 1712–1716
31. Bhasin A, Bommavaram R, Greenfield M L, Little D N. Use of molecular dynamics to investigate self-healing mechanisms in asphalt binders. Journal of Materials in Civil Engineering, 2011, 23(4): 485–492
32. Xu G, Wang H. Molecular dynamics study of oxidative aging effect on asphalt binder properties. Fuel, 2017, 188: 1–10
33. Guo M, Tan Y, Wei J. Using molecular dynamics simulation to study concentration distribution of asphalt binder on aggregate surface. Journal of Materials in Civil Engineering, 2018, 30(5): 04018075
34. Wang P, Zhai F, Dong Z, Wang L, Liao J, Li G. Micromorphology of asphalt modified by polymer and carbon nanotubes through molecular dynamics simulation and experiments: Role of strengthened interfacial interactions. Energy & Fuels, 2018, 32(2): 1179–1187
35. Ding Y, Huang B, Shu X, Zhang Y, Woods M E. Use of molecular dynamics to investigate diffusion between virgin and aged asphalt binders. Fuel, 2016, 174: 267–273
36. Li R, Du H, Fan Z, Pei J. Molecular dynamics simulation to investigate the interaction of asphaltene and oxide in aggregate. Advances in Materials Science and Engineering. 2016, 2016: 3817123
37. Sun H. COMPASS: An ab initio force-field optimized for condensed-phase applications overview with details on alkane and benzene compounds. Journal of Physical Chemistry B, 1998, 102(38): 7338–7364
38. van Duin A C, Dasgupta S, Lorant F, Goddard W A. ReaxFF: A reactive force field for hydrocarbons. Journal of Physical Chemistry A, 2001, 105(41): 9396–9409
39. Pan T, Lu Y, Lloyd S. Quantum-chemistry study of asphalt oxidative aging: An XPS-aided analysis. Industrial & Engineering Chemistry Research, 2012, 51(23): 7957–7966
40. Kmiecik S, Gront D, Kolinski M, Wieteska L, Dawid A E, Kolinski A. Coarse-grained protein models and their applications. Chemical Reviews, 2016, 116(14): 7898–7936
41. Marrink S J, Risselada H J, Yefimov S, Tieleman D P, De Vries A H. The MARTINI force field: Coarse grained model for biomolecular simulations. Journal of Physical Chemistry B, 2007, 111(27): 7812–7824
42. Arash B, Park H S, Rabczuk T. Mechanical properties of carbon nanotube reinforced polymer nanocomposites: A coarse-grained model. Composites. Part B, Engineering, 2015, 80: 92–100
43. Materials Studio. Version 8.0. San Diego, CA: Biovia Inc., 2014
44. Artok L, Su Y, Hirose Y, Hosokawa M, Murata S, Nomura M. Structure and reactivity of petroleum-derived asphaltene. Energy & Fuels, 1999, 13(2): 287–296
45. Yao H, Dai Q, You Z. Molecular dynamics simulation of physicochemical properties of the asphalt model. Fuel, 2016, 164: 83–93
46. Siddique R, Naik T R. Properties of concrete containing scrap-tire rubber—An overview. Waste Management, 2004, 24(6): 563–569
47. Tanaka Y. Structural characterization of natural polyisoprenes: Solve the mystery of natural rubber based on structural study. Rubber Chemistry and Technology, 2001, 74(3): 355–375
48. Sun D, Lin T, Zhu X, Tian Y, Liu F. Indices for self-healing performance assessments based on molecular dynamics simulation of asphalt binders. Computational Materials Science, 2016, 114: 86–93
49. Read J, Whiteoak D. The Shell Bitumen Handbook. Thomas Telford, 2003

50. Li D D, Greenfield M L. Chemical compositions of improved model asphalt systems for molecular simulations. Fuel, 2014, 115: 347–356
51. Argyris D, Cole D R, Striolo A. Dynamic behavior of interfacial water at the silica surface. Journal of Physical Chemistry C, 2009, 113(45): 19591–19600
52. Wool R, O'connor K. A theory crack healing in polymers. Journal of Applied Physics, 1981, 52(10): 5953–5963
53. Schapery R. Nonlinear fracture analysis of viscoelastic composite materials based on a generalized J integral theory. In: Kawata K, Akasak T, eds. Japan-U.S. Conference on Composite materials: Mechanics, mechanical properties and fabrication. Tokyo: Japan Society for Composite Materials Tokyo, 1982: 171–180
54. Gao Y, Zhang Y, Gu F, Xu T, Wang H. Impact of minerals and water on bitumen-mineral adhesion and debonding behaviours using molecular dynamics simulations. Construction & Building Materials, 2018, 171: 214–222
55. Frenkel D, Smit B. Understanding Molecular Simulation: From Algorithms to Applications. Academic Press: New York, 2002
56. Lv Q, Huang W, Xiao F. Laboratory evaluation of self-healing properties of various modified asphalt. Construction & Building Materials, 2017, 136: 192–201